

1 **Limited specificity of molecular interactions incurs an environment-**
2 **dependent fitness cost in bacteria**

3 Claudia Iglér^{1,2}, Claire Fourcade¹, Torsten Waldminghaus³, Florian M. Pauler¹, Balaji Santhanam⁴,

4 Gašper Tkačik¹, Călin C. Guet^{1,*}

5

6 ¹ IST Austria, Am Campus 1, 3400 Klosterneuburg, Austria

7 ² Institute of Integrative Biology, Universitätsstrasse 16 ETH Zurich, 8092 Zurich, Switzerland

8 ³ Department of Biology, Technische Universität Darmstadt, Darmstadt, Germany

9 ³ Centre for Synthetic Biology, Technische Universität Darmstadt, Darmstadt, Germany

10 ⁴ Department of Systems Biology, Columbia University,

11 1150 St. Nicholas Avenue, New York, NY 10032

12

13 * Corresponding author: Călin C. Guet

14 **Email:** calin@ist.ac.at

15

16 **Competing Interest Statement:** There are no competing interests.

17 **Classification:** Biological Sciences/ Microbiology

18 **Keywords:** Transcription factors, DNA binding, limited binding specificity, binding cooperativity

19

20

21

22 **Abstract**

23 Reliable operation of cellular programs depends crucially on the specificity of biomolecular
24 interactions. In gene regulatory networks, the appropriate expression of genes is determined through
25 the specific binding of transcription factors (TFs) to their cognate DNA sequences. However, the large
26 genomic background likely contains many DNA sequences showing similarity to TF target motifs,
27 potentially allowing for substantial non-cognate TF binding with low specificity. Whether and how non-
28 cognate TF binding impacts cellular function and fitness remains unclear. We show that increased
29 expression of different transcriptional regulators in *Escherichia coli* and *Salmonella enterica* can
30 significantly inhibit population growth across multiple environments. This effect depends upon (i) TF
31 binding to a large number of DNA sequences with low specificity, (ii) TF cooperativity, and (iii) the
32 ratio of TF to DNA. DNA binding due to the limited specificity of promiscuous or non-native TFs can
33 thus severely impact fitness, giving rise to a fundamental biophysical constraint on gene regulatory
34 design and evolution.

35

36 **Introduction**

37 Biology at all levels crucially depends on the timely recognition and interaction between cognate
38 biomolecules (Box 1A). The importance of specificity of molecular encounters in the cell is highlighted
39 by the intricate mechanisms that ensure appropriate, and thus specific interactions, a classic example
40 being kinetic proofreading in the loading of amino acids onto tRNAs (1). In gene regulation,
41 transcription factors (TFs) determine the expression of genes at the right time and place by binding to
42 their respective operator sites in a highly specific manner. Additionally, non-cognate interactions can
43 occur due to non-specific TF-DNA interactions or due to specific binding (i.e. recognition of a TF-
44 specific DNA motif) at non-cognate sites (Box 1). These interactions are not necessarily detrimental,
45 as non-specific DNA binding was found to speed up the TF search process through sliding along the
46 DNA (called “facilitated diffusion”) (2,3). Upon encounter of the target sequence, conformational
47 changes can then increase binding specificity (2). In prokaryotes, many transcriptional regulators
48 appear to be non-specifically bound to DNA most of the time (3,4) and this state likely plays an
49 important role in gene regulation (5–7).

50

51 These non-specific TF-DNA interactions are likely weak and transient. However, non-cognate TF-
52 DNA interactions can also arise from recognition of a certain DNA motif or conformation, which makes
53 them more specific and therefore stronger (Box 1). As TFs have to search for their ‘correct’ DNA
54 targets among an extensive genomic background, they might encounter many non-cognate sites with
55 sufficient target sequence similarity, thus potentially trapping TF molecules (2,8). TF binding to such
56 non-cognate sites could thus incur substantial fitness consequences for the cell through i) high-
57 specificity binding to few DNA sites with high similarity to the target sequence ; or ii) low-specificity
58 binding to many sites across the genome that accrues to a large overall effect. While in i) the fitness
59 effect is more likely to stem from regulatory interference, in ii) also changes in chromosome structure
60 could play a role. In support of the latter, growth arrest has been found with overexpression of one of
61 the nucleoid-associated proteins (NAPs) of *E. coli* involved in DNA organization, H-NS (9), which
62 binds DNA preferentially at AT-rich and curved regions (10).

63

64 In eukaryotes, which have shorter operator sites, low-specificity non-cognate binding of TFs seems to
65 be an integral part of gene regulatory function and evolution (11,12). On the other hand, in a recent
66 theoretical study that explored the impact of non-cognate binding we suggested that genomic low-
67 specificity sites impose the existence of a global biophysical constraint, termed “crosstalk” (13). Some
68 forms of TF cooperativity and combinatorial regulation can limit this problem (13), but additional
69 mechanisms, such as out-of-equilibrium proofreading mechanisms, may be at work as well in
70 eukaryotes (14,15). In prokaryotes, the importance of non-cognate binding with low specificity has
71 rarely been investigated, although it has been acknowledged in regulatory interference (16), however
72 experiments exploring its fitness impact in general are lacking entirely.

73

74 **Results**

75 ***Experimental setup***

76 We wanted to test the consequences of non-cognate TF binding on bacterial fitness by expressing
77 TFs lacking known cognate binding sites in native and non-native host cells. For this purpose, we
78 chose phage repressors, which coexist for long periods at low numbers in bacterial hosts during the
79 lysogenic cycle. We expect these repressors to be adapted to their host’s genomic background – as
80 temperate phages likely spend most of their existence as lysogens (17) – but potentially not to that of

81 another host. Therefore, we use repressors from different lambdoid phages, but from the same
82 protein family, three of them native to *E. coli* (λ *cl*, 434 *cl*, HK022 *cl*) and one to *S. enterica* (P22 *c2*)
83 and explore their effects on growth and fitness in both bacterial hosts. A bacterial repressor, LacI,
84 served as a control in our experiments, as it is known to have only a single cognate target region in *E.*
85 *coli*, at the *lac* operon (18). Further, LacI uses facilitated diffusion for target search (3), which means it
86 should have very weak non-specific binding tendencies that should not affect fitness. Note, that all
87 four phage transcriptional regulators can function as either repressors or activators depending on the
88 promoter they bind to.

89 The five repressors were each cloned under the control of an aTc-inducible promoter (P_{tet}) onto a low
90 copy number plasmid (Fig. 1A). The plasmids were then transformed into *E. coli* and *S. enterica* cells,
91 whose genomes do not contain any of the phage operators, nor the three *lac* operators. The phage
92 repressors bind to their cognate operator sites in the phage genome as a dimer, but they can also
93 bind cooperatively to adjacent operators or form short- and long-distance loops (up to 10kbp for λ CI
94 (20)) involving two to four dimers (21) (Fig. 1A). This type of TF cooperativity was previously found to
95 facilitate non-cognate binding (22). Notably, for λ CI significant non-cognate binding has been
96 predicted theoretically (22,23) and substantiated experimentally (24), whereas for P22 C2 binding was
97 lost at few mismatches with the target motif (24), making it a less likely non-cognate binder (Box 1B).
98 LacI on the other hand, is a tetrameric protein and cooperativity stems from the fact that one
99 repressor tetramer can bind to two different DNA sites simultaneously, resulting in looping (25), as
100 opposed to cooperativity resulting from binding of two different repressor molecules (Fig. 1A), which
101 LacI lacks. We compared the impact of potential low-specificity non-cognate interactions of the five
102 different TFs by measuring growth of *E. coli* and *S. enterica* in various environments over a 10h
103 interval as a fitness proxy.

104

105 ***Repressor-induced growth reduction depends on growth medium and induction timing***

106 Reduction in growth was quantified as the normalized difference between growth in the presence and
107 absence of repressor (with 1 indicating complete cessation of growth and 0 representing wildtype
108 growth, see Methods). We observed a wide spectrum of growth behaviors across the five repressors
109 and the two bacterial hosts. For cells grown in minimal media (M9) with glucose (the standard media
110 used if not specified otherwise), the presence of λ CI resulted in a strong reduction of growth in *E. coli*

111 and an even more substantial reduction in *S. enterica* cells (Fig. 1B-D, Table S1). 434 CI also
112 reduced growth in both hosts, though less than λ CI, and interestingly more in its native host, *E. coli*
113 (Fig. 1B). P22 C2 on the other hand, showed no effect in its native host *S. enterica*, while stopping
114 growth completely when expressed in *E. coli* (Fig. 1D, Table S1). There was no significant impact on
115 growth in either host with HK022 CI or with Lacl (Fig. 1B), which was expected for the latter - at least
116 in *E. coli*. Further, no growth defect was seen with our other controls: cells with only plasmid
117 backbone or the control plasmid expressing a fluorescence marker instead of a repressor (Fig. S1A).
118 Thus, four different repressors stemming from the same TF family, but likely having different modes of
119 DNA recognition (26), showed a broad spectrum of growth effects in the two different bacterial host
120 species. We explored these growth effects and their causes further by focusing on the two best-
121 characterized ones, λ CI and P22 C2, which are known to have different propensities for binding at
122 DNA sequences far away from their target motif (24) (Box 1B).

123

124 As a next step, we varied the environmental conditions in which bacteria carrying λ CI or P22 C2 were
125 grown. In rich media (LB), growth inhibition was abolished almost entirely in *E. coli* for both
126 repressors, and substantially reduced with λ CI expressed in *S. enterica* (Fig. 2A, Table S1). Minimal
127 media supplemented with casamino acids and glucose resulted in intermediate growth reductions
128 between rich and poor media (Fig. S2A, Table S1). P22 C2 did not affect growth in *S. enterica* in any
129 of the conditions (Fig. 2A, Table S1), which is why this combination is generally not discussed further.

130

131 Next, we tested the dependence of the growth reduction on repressor concentration and induction
132 timing. In *E. coli*, decreasing the concentration of either repressor showed a gradual recovery of
133 normal growth (Fig. 2B, Table S2). Conversely, even low expression of λ CI in *S. enterica* resulted in
134 strong growth reductions (Fig. 2B, Table S2). The concentrations used here (see Methods for
135 measurement details) range from 0.5-5 fold of those achieved under physiological lysogen conditions
136 (27). Surprisingly, the induction time point was also an important determinant for λ CI-induced growth
137 reduction, not however for P22 C2-induced ones: while λ CI induction in early- and mid-exponential
138 growth (as opposed to induction during the lag phase) had progressively smaller effects on growth in
139 *E. coli* and *S. enterica* (Fig. 2C, S2B,C, Table S3), this was not the case for P22 C2 in *E. coli*, where
140 growth was always halted ~2h after repressor induction (Fig. S2D, Table S3). Overall, we found a

141 strong dependence of repressor-induced growth reduction on environmental conditions and repressor
142 concentration.

143

144 ***Increased repressor expression leads to severe fitness reduction***

145 As the severe growth reductions we observed made it difficult to determine meaningful growth rates in
146 our system, we determined the fitness effect of repressor expression in direct competition
147 experiments, which reflect all growth differences between the competitors. As a 'neutral' competitor,
148 we used cells expressing LacI from a plasmid construct that contained an additional YFP-*venus*
149 marker (Fig. 3A). The *venus* marker resulted in a minor fitness cost (selection coefficients for cells
150 without the marker were 0.05 (*E.coli*) and 0.09 (*S.enterica*), see Methods), meaning that an increase
151 in fluorescence (i.e. LacI-carrying cells) indicates an even more pronounced benefit of the LacI-
152 carriers than measured. 1:1 mixtures of cells with phage repressor- and LacI-carrying plasmids were
153 grown in minimal media (Fig. 3A, Methods) and fluorescence was compared between cell mixtures
154 grown without the repressors (no fitness difference; baseline fluorescence) and cell mixtures induced
155 for repressor expression (potential fitness cost of phage repressors over LacI) (28). In accordance
156 with the experimental results from Fig. 1B-D, expression of repressors led to a significant increase in
157 LacI-expressing cells, except for competitions with P22 C2 in *S. enterica* (Fig. 3B,C, Table S4).
158 Growth reductions translated directly into fitness costs as the competition assays were even able to
159 capture the gradual increase in growth reduction with increasing repressor concentration for λ CI in *S.*
160 *enterica* (Fig. S3, Table S4).

161

162 ***Growth reduction is caused by cooperative, low-specificity binding distributed across the*** 163 ***genome***

164 Given the surprisingly detrimental growth effect of the two repressors in several environments, we set
165 out to determine its cause. Transcriptional repressors are DNA-binding proteins and could therefore
166 interfere with the cellular program through DNA binding at various non-cognate sites (29). To
167 determine the role of TF binding in the observed growth reductions, we used the fact that λ CI is one
168 of the best-studied TFs, and thus an exhaustive range of mutants for most of its functions exist. As
169 neither of these mutants have been characterized for any of the other repressors, we only performed
170 these experiments with λ CI.

171

172 Specifically, we tested the expression of a mutant that cannot form dimers (30) (as λ CI only binds
173 DNA in its dimeric form (31)), as well as of a mutant defective in DNA binding (32), and found that
174 normal growth (Fig. 4A, Table S3) and fitness (Fig. S3) were almost completely restored in *E. coli* as
175 well as in *S. enterica* cells. Similar results for a λ CI mutant defective in cooperativity between
176 repressor dimers (Fig. 4A, Table S3) suggest an important contribution from DNA looping or some
177 other form of repressor oligomerization. This is intriguing as λ CI cooperativity and oligomerization are
178 thought to increase binding specificity (25,33), but likely lead to a general increase in binding strength,
179 particularly in the absence of specific sites. We ruled out that repressor misfolding or aggregation was
180 responsible for our observations by over-expressing a chaperone gene (*tig*) together with the
181 repressors (Fig. S1B).

182

183 Hence, the ability to bind DNA, potentially in a cooperative and motif-dependent manner, seems to be
184 central to repressor-mediated growth effects. We tested this hypothesis by combining λ CI
185 cooperativity with the binding specificity of another repressor, using chimeric TFs. Specifically, we
186 replaced the DNA binding helix of λ CI (see Methods) with: i) that of another phage repressor, 434 CI,
187 which showed some growth defect; and ii) the bacterial repressor, LacI, which showed no growth
188 defect as a wildtype protein (Fig. 1B, Table S5). It has been reported that changes in the geometry of
189 434 CI cooperativity strongly interfere with its binding affinity and the structure of the TF-DNA complex
190 (21,34), which indeed in our experiments resulted in rescue of growth with the λ -434 CI chimera. In
191 contrast, with the λ CI-LacI chimera the growth reductions were even stronger than with λ CI, leading
192 to growth arrest in *S. enterica* in rich and minimal media (Fig. 4B, Table S5). This opposing behavior
193 of LacI and λ CI-LacI strongly supports our hypothesis that LacI binding affinity and basepair bias are
194 conducive to low-specificity binding (Box 1B), but it is lacking the strong intermolecular cooperativity
195 and oligomerization potential of λ CI (Fig. 1A). The chimera, however, combines these attributes,
196 leading to strong interference with cell growth.

197

198 In order to determine if the non-cognate binding effects involved (i) a few essential, or (ii) many
199 distributed, regions of the chromosome we performed ChIP-sequencing for λ CI in *E. coli* and *S.*
200 *enterica*. In *E. coli* the data did not reveal strong peaks for any genomic site, but rather indicated weak

201 binding at numerous sites all over the chromosome (Fig. 5A, S4A, Table S6). Note that all of the
202 regions plotted in Fig. 5A are significantly enriched in the presence of λ CI, but they only appear at a
203 more lenient cutoff than typically used for strong binding (see Methods). In *S. enterica* we found both,
204 distributed weak binding as well as a broad peak (indicating substantial binding in several adjacent
205 genes). Interestingly, this broad peak corresponds to prophage regions on the genome that seem to
206 provide binding hotspots for λ CI (Fig. 5B, S4B, Table S6). As such a binding hotspot was absent in *E.*
207 *coli*, but λ CI still showed a growth defect, we did not consider this finding necessary to qualitatively
208 explain our results (although it could account for the stronger growth defects seen in *S. enterica*).
209 Further, none of the apparent peaks for either genome encoded a gene that is essential or obviously
210 beneficial in minimal media conditions.

211

212 Using a simple thermodynamic model to predict λ CI binding across the bacterial genome we found a
213 surprisingly high degree of correlation with the number of reads from ChIP-seq (Fig. 5C,D),
214 especially given that these models generally perform poorly for low affinity sites (35). Even more
215 surprising, we found a comparable prediction (Fig. 5C,D, S5) with an energy matrix that conserved
216 only the overall λ CI preference for the basepair composition (see Methods). This result could not be
217 explained by nucleotide composition bias in the ChIP-seq experiments (Fig. S6), but shows
218 that a large part of the correlation between predicted binding and ChIP-seq reads can be
219 explained by the overall genomic basepair bias. Correct basepair composition bias in the DNA
220 sequences could provide λ CI with sufficient recognition pattern to bind with low specificity. In
221 agreement with this hypothesis, the GC bias of the stronger λ CI cognate operators (O_{R1} , O_{R2} , O_{L1} and
222 O_{L2}) is 52.94%, which is very close to that of the *S. enterica* genome (52.2%) and only slightly higher
223 than that of the *E. coli* genome (50.8%). However, the residual sequence-dependent contribution
224 beyond the basepair composition bias is still highly significant in *E. coli* and weakly significant in *S.*
225 *enterica* (as determined by Monte-Carlo permutation tests for significance; Fig. 5C,D, S7). Overall,
226 our results indicate substantial non-cognate binding due to sequence-dependence and basepair bias,
227 which has been also reported, for example, for NAPs (9,10). Non-cognate binding is facilitated by
228 repressor oligomerization (22,36), and distributed over the thousands of low-specificity λ CI binding
229 sites, known to be present in the *E. coli* genome (29). These findings agree with previous studies on
230 non-cognate binding of λ CI and other prokaryotic TFs (2,3,23,37).

231

232 ***Low-specificity binding leads to arrest of cell division***

233 The distributed non-cognate DNA binding demonstrated by the ChIP-sequencing data for λ CI is in
234 agreement with the observation that increasing concentrations of repressor gradually increases the
235 magnitude of the growth reduction seen in Fig. 2B. Additionally, the dependence on growth media and
236 induction timing indicates that DNA concentration – or rather the ratio between repressor and DNA –
237 might play a role. If cell doubling time is slower than the time needed for DNA replication and cell
238 division (~60min. in *E. coli* (38) and ~50min. in *S. enterica* (39), which is close to our observed
239 doubling time in minimal media: ~63min. and ~58min. respectively), each bacterial cell contains on
240 average only one chromosome. At faster growth, replication cycles are overlapping and daughter cells
241 inherit 2-8 origins at birth, together with partially replicated chromosomes (38). Hence, the richer the
242 medium and the faster the growth, the more DNA will be available (~2-fold for rich versus minimal
243 media in our experiments) to titrate away potentially detrimental non-cognate binding TFs. In
244 agreement with previous studies (40), the number of proteins at fast and slow growth were very
245 similar (see Methods: Protein quantification), leading to a decreased protein concentration in rich
246 media as cells become larger (this is particularly true for proteins expressed from plasmids (40)).
247 Similarly, cells that are induced during the lag or early-exponential phase (after 1-2 doublings) will
248 only have on average one chromosome as they did not inherit partially replicated chromosomes from
249 their mothers and grandmothers yet.

250

251 Thus we set out to test the titration hypothesis by introducing a high copy number plasmid carrying
252 four cognate λ CI binding sites into *E. coli* cells with inducible λ CI (Fig. S8A), which should reduce the
253 number of free λ CI dimers available for non-cognate binding by about one half (see Methods).
254 Although the expression of λ CI was still detrimental, growth was ~20% faster than for cells without
255 the operators (Fig. S8B). Hence, titration of λ CI alleviates the growth reduction – likely even more so
256 if additional chromosomal DNA is present (e.g. at faster growth), which provides many more potential
257 binding sites with low specificity (29). For P22 C2, which is more discerning in its DNA binding targets
258 (24), partially replicated chromosomes would provide less titration, thus explaining why later induction
259 does not rescue growth. The titration phenomenon is reminiscent of growth bistability in drug resistant
260 bacterial cells, which is caused by feedback between the growth rate and the speed of counteracting

261 toxic agent (41). In our system, the repressors can be seen as ‘toxic agents’, which are ‘counter-
262 acted’ by dilution if cells manage to start growing, or are growth-arrested if they are not able to dilute
263 the repressors fast enough.

264

265 The titration hypothesis together with our ChIP-sequencing results implies that the overall ratio of
266 chromosomal DNA to repressor proteins is a crucial factor determining the growth effects. This
267 suggests that non-cognate binding might interfere with global cellular functions, like DNA replication
268 or cell division, which we investigated using fluorescence microscopy of *E. coli* cells expressing λ CI.
269 First, we imaged cells expressing a SeqA-GFP fusion protein, which is an indicator of replication fork
270 progression (42). λ CI-expressing cells generally formed long filaments, suggesting an inhibition of
271 cell division in these cells, even though the numerous fluorescent dots revealed ongoing replication
272 (Fig. 6A, S9). Most filamentous cells showed low induction of the stress response promoter *PsulA*
273 (Fig. 6B, S10), which is unlikely to induce sufficient self-cleavage (i.e. inactivation) of the repressor
274 molecules (43) - particularly because λ CI becomes a poor substrate for self-cleavage at higher
275 concentrations (44) - or to inhibit cell division substantially (45). Cell division can also be hindered by
276 the presence of DNA at mid-cell (46). Fluorescence microscopy of cell membrane and DNA shows
277 that in many filamentous cells DNA is located mid-cell, often on top of the established division septum
278 (Fig. 6C, S11). This suggests that it is not FtsZ-ring formation, but a subsequent step in the cell
279 division cascade that is disrupted. However, some filamentous cells manage to divide after growing to
280 substantial length, as FtsZ-ring formation starts to occur at quarter points (47). Indeed,
281 overexpression of FtsZ together with λ CI rescues growth entirely (Fig. S12), likely by forming
282 additional, non-central division septa, which could produce viable cells as filamentous cells often
283 contain additional chromosomes, which are distributed across the cell (Fig. 6C). As the *ftsZ* operon
284 region was not enriched among ChIP-sequencing reads, it is unlikely that λ CI interferes with FtsZ
285 expression directly through transcriptional interference.

286

287 **Discussion**

288 We investigated the consequences of limited specificity in molecular recognition of DNA by proteins,
289 using four different, but related, phage repressors and a bacterial repressor, which produced a wide
290 range of effects on host cell growth, from high to no fitness costs, and higher costs either in the native

291 or the non-native host (Fig. 1B, 4B). Taking advantage of the rich and well-established genetics and
292 biochemistry of the classic bacteriophage repressor λ CI, we found that its fitness cost results from
293 cooperative, low-specificity binding, which interferes with growth by inhibiting cell division. The
294 abundance of low-specificity binding sites in eukaryotic genomes has been shown to play a critical
295 role in gene regulation, potentially increasing robustness and specificity (11). Our data, however,
296 support the hypothesis that binding strategies of prokaryotic TFs are under selection to avoid low-
297 specificity binding to the genomic background (29) and highlight the fundamental differences in gene
298 regulatory design between prokaryotes and eukaryotes, and therefore differing evolutionary
299 constraints (48).

300

301 For prokaryotes – in contrast to eukaryotes – TF target sites are sufficiently long to allow specific
302 recognition of single operators (48). Mismatches with the preferred target sequence lead to
303 progressive loss of binding, but the speed of this loss can vary substantially between TFs (24). λ CI,
304 which shows strong operator binding (offset), low mismatch penalties (energy matrix) and strong
305 cooperativity, is likely to be a rather promiscuous binder (Box 1B, (24)) and indeed induced a high
306 fitness cost due to distributed low-specificity binding. For P22 C2, the lower offset and higher
307 mismatch penalties make it a more specific binder (Box 1B, (24)), producing a significant cost only in
308 non-native host cells. Lacl, which shows similar binding characteristics as λ CI, only showed a strong
309 fitness effect when coupled with λ CI's intermolecular cooperativity. Together, the mutant and chimera
310 experiments (Fig. 4) demonstrate a significant contribution of cooperativity - and likely oligomerization
311 - to the potential for low-specificity binding, which supports the theoretical finding that TF cooperativity
312 does not strongly alleviate crosstalk when it stabilizes cognate as well as non-cognate binding (13).
313 Hence, the lack of intermolecular cooperativity with Lacl could be a sign of its adaptation to be highly
314 specific, as it is one of the few single-target regulators in *E. coli* (18). Binding cooperativity, offset and
315 TF concentration, can all serve to increase non-cognate binding of a TF (independently of the target
316 motif preference) and the particular interplay between these factors has to be tuned by the cell to
317 avoid fitness costs due to low-specificity interactions. Therefore, considering low-specificity binding is
318 crucial in choosing TFs for synthetic biological systems in order to avoid global toxicity effects, as well
319 as unwanted TF titration, which can affect target gene regulation (16,49).

320

321 The magnitude of the fitness cost depends on a repressor's ability to bind non-cognate DNA at low
322 specificity, as well as on a repressor's relative ratio to the total amount of DNA within the cell. Slow
323 cell growth compounds the effect as cells contain less DNA but accumulate more proteins than at fast
324 growth (40). Additionally, stress tolerance could be higher under optimal growth conditions as found in
325 rich media (50). It does not seem likely, however, that media-specific genes are targeted, as ChIP-
326 sequencing generally revealed distributed, low-specificity binding all over the chromosome (Fig. 5).
327 Rather, inhibition of cell division seems to result at least partially from nucleoid localization at mid-cell.
328 Clearance of the division site is impeded if sister chromosomes fail to segregate (46,51), which could
329 be caused by the formation of "bridges" between cooperatively bound repressors, holding the sister
330 chromosomes together. Generally, more compact nucleoids are more efficient at preventing the
331 formation of division septa in the same area (52). Intriguingly, a very similar growth effect has been
332 found with H-NS, one of the NAPs responsible for chromosome organization and compaction in *E.*
333 *coli* (9,10): H-NS overproduction drastically reduced cell viability, which seemed to be related to the
334 formation of higher-order H-NS oligomers (53) – a state that is favoring its ability to form bridges
335 between DNA regions (54). As cell growth, shape, division and DNA replication are thought to be
336 tightly linked in complex and poorly understood ways (55), a mechanistic explanation of the observed
337 division inhibition is presently not possible, but prior studies on H-NS combined with our findings
338 make the case for the existence of general constraints on DNA-binding proteins.

339

340 Our results suggest that the inherent ability of DNA-binding proteins to occupy non-cognate DNA
341 regions can pose, in addition to potential regulatory interference (16), a substantial challenge for host
342 cell fitness overall – particularly considering facilitating conditions like cellular crowding (56),
343 horizontal gene transfer (57) and mutations that alter the binding specificity of a protein. This
344 challenge stems from the fundamental limits to molecular recognition that are set by the biophysics of
345 molecular interactions (13) and could lead to various non-cognate effects on the physiology of the
346 cell. The five transcription factors used here show a variety of non-cognate effects, which could
347 indicate different selection pressures that have been acting on their binding and cooperativity
348 characteristics as well as different potential for being tolerated in a particular environment. There
349 might also be different mechanisms underlying the growth phenotype, as suggested by the ChIP-
350 sequencing results for λ CI: the additional strong peak region found in *S. enterica* could indicate an

351 additional effect of high-affinity sites and explain the stronger growth defect as compared to *E. coli*
352 (especially at low repressor concentrations). A potential for high fitness costs, even in native
353 environments, as seen here with λ CI and 434 CI, can limit the number and binding affinity of
354 promiscuous DNA-binding proteins in the cell (13). More specific binders such as P22 C2 might only
355 be detrimental in non-native environments. Hence, the influx of foreign genes through horizontal gene
356 transfer could be considerably impaired through non-cognate binding effects, as both are likely to
357 occur under slow growth conditions. As the phage repressors we used originate from temperate
358 phages, interference with host cell growth can limit their potential host range with regard to
359 successfully establishing lysogeny. Considering that phage repressor concentrations are kept low
360 during lysogenic cycles, the selection pressure to reduce low-specificity binding might generally be
361 weak, which would explain the diversity in fitness impacts we observed with related phage repressors.
362 More generally, experimentally uncovering the fundamental biophysical constraints imposed by low-
363 specificity bindings of TFs is difficult, as TFs with many specific binding targets need to recognize a
364 diversity of sequences and by default affect many cellular functions, while single target TFs are a very
365 few (18). This is what ultimately motivated our choice of focusing our experiments on phage
366 repressors and LacI.

367

368 We experimentally demonstrated for the first time that low specificity in biomolecular recognition can
369 constitute a limiting factor for cellular function and evolution due to the fundamental biophysical
370 constraints on protein-DNA interactions. However, these costs could be counter-balanced by
371 increased TF robustness to target site mutations or higher evolvability, precisely because interactions
372 can be formed at low specificity (24,58). For example, a TF could co-opt regulation of a non-cognate
373 gene - even if only to a small degree - that provides an advantage in a certain environment, which
374 can subsequently be refined by evolution. This opens up a wider question about the interplay of costs
375 and benefits of low-specificity molecular interactions, especially when these interactions also serve as
376 drivers of evolution.

377

378 **METHODS**

379 *Plasmids and strains*

380 The phage repressors λ CI, P22 C2, 434 CI, HK022 CI or the bacterial repressor LacI were cloned
381 under the control of a $P_{LtetO-1}$ promoter in a low copy number *kan^R* plasmid (pZS)(59). The plasmids
382 were then transformed into either MG1655 derived *E. coli* cells, which are deleted for the *lac* operon

383 (strain BW27785, CGSC#: 7881)(60), or into LT2 derived *S. enterica* cells with a tetracycline cassette
384 inserted in the P22 attachment site (LT2 attP22::*tetRA*). In control experiments the phage repressor
385 on the plasmid was replaced by a fluorescence marker gene (*gfp*). The low copy number plasmids
386 used (pZS21) are under stringent replication control, which is linked to chromosome replication (61).
387 Titration of λ CI was tested by transforming *E. coli* cells containing the pZS21- λ *ci* plasmid with a
388 compatible, high-copy number pZE plasmid (50-70 copies)(59), which carries the natural λ CI
389 operators O_{R1} , O_{R2} , O_{L1} and O_{L2} , i.e. 200-280 operators per cell – although the copy number of this
390 plasmid's ori was originally documented at 25-30 copies per cell (62), hence there might only be
391 about 100-120 operators per cell. At 25ng aTc induction, there are about 500 λ CI dimers per cell (see
392 below), which reduces the number of dimers available per cell either by half or by one fifth.
393 For the competition experiments we introduced a constitutive fluorescent marker *venus-yfp* (63) into
394 the low-copy pZS plasmid carrying *lacI* (for a detailed description see below).
395 In order to test for misfolding of repressor proteins, we used a high copy number plasmid containing a
396 chaperone gene (*tig* (64)), which is native to *E. coli* and *S. enterica*, under the control of a P_{Lac}
397 promoter from the ASKA(-) library (65).
398 To monitor induction of the stress response, we used a strain with a fast-maturing yellow fluorescent
399 protein (YFP)(63) fused to the promoter of *sulA* (*PsulA-yfp*), which was placed on the chromosome
400 using lambda red recombineering (66). *SulA* is strongly upregulated as a part of the stress response
401 (67). The *PsulA-yfp* strain was then transformed with the pZS21- λ *ci* plasmid. We checked induction
402 of the reporter by exposing cells to UV light for 30 seconds.
403 We used a SeqA-GFP translational fusion under the control of the natural *seqA* promoter to monitor
404 replication as SeqA binds hemi-methylated GATC sequences in the wake of the advancing replication
405 fork, marking newly synthesized DNA (42). In order to avoid unnaturally high *seqA* expression that
406 could influence replication progression, the fusion protein was inserted into the HK022 attachment site
407 on the *E. coli* chromosome using CRIM plasmids (68).
408 Additional expression of FtsZ, the major cell division protein, was performed by cloning *ftsZ*
409 downstream of λ *ci* as a transcriptional fusion (i.e. putting it also under the control of aTc induction).

410

411 λ CI mutants

412 Based on previous studies, we cloned three different λ repressor mutants into the same low copy
413 number plasmid (pZS) under the control of a $P_{LtetO-1}$ promoter: (i) a repressor mutant that is defective
414 in its ability to bind DNA (N52D)(32); (ii) a repressor mutant that cannot form dimers (S228N)(30) and
415 hence not bind DNA effectively anymore; and (iii) a mutant that can dimerize but not form higher-order
416 oligomers, i.e. that cannot bind cooperatively (Y210N)(30). Mutations were introduced using site-
417 directed mutagenesis. The function and stability of the proteins has been shown previously (30,32),
418 as well as that their production levels are not different from wildtype repressor (30).

419

420 λ CI chimeras

421 Chimeric λ CI repressors were constructed based on literature describing a chimeric λ CI-434
422 repressor (69) and a chimeric 434-P22 repressor (70) by changing the recognition (i.e. DNA binding)

423 helix of λ CI to either the one of the 434 CI repressor or of the LacI repressor. This was done by
424 introducing the following changes for the λ CI-434 chimera: G44T, S46Q, G49E, A50Q; and for the λ
425 CI-LacI chimera: G44S, Q45Y, S46Q, G49S, A50R. (Note, that Q45 was not changed in the λ CI-434
426 chimera because both repressors contain the amino acid Q at this position.)

427

428 *Growth measurements*

429 All cells were grown overnight at 37°C in M9 medium supplemented with 0.2% glucose and 50 μ g/ml
430 kanamycin (except specified differently). Cultures were used to dilute (1:100) 6 replicates without
431 inducer and 6 replicates with 25ng aTc in 96 well plates and were grown at 37°C under shaking at
432 220 rpm. Populations were measured (OD₆₀₀) every 30min or every 60min using Biotek H1 plate
433 reader for 10h. Population growth was also measured in LB, or M9 medium supplemented with 0.5%
434 Casamino acids and either 0.5% glycerol or 0.2% glucose. Where indicated inducer concentration
435 was changed to 1, 2, 3 and 4ng aTc - which was chosen in a way that the concentration range was
436 covered as uniformly as possible, given that the $P_{LtetO-1}$ promoter has a very steep induction curve
437 (59) - and the induction time was varied from the inoculation time point (0h) to 2h or 4h post-
438 inoculation (early- and mid-exponential phase). The chaperone gene was induced using 1mM IPTG
439 and Fis-GFP was expressed by adding 0.1mM IPTG to the medium.

440 Growth reduction was measured as the normalized difference between the areas under the growth
441 curves (from the point of induction for 8.5h, i.e. including lag phase but not stationary growth) in the
442 presence and absence of repressor ($\frac{AUC_{no\ repressor} - AUC_{repressor}}{AUC_{no\ repressor}}$). Hence, a ratio of 0 corresponds to
443 wildtype growth even in the presence of repressor and a ratio of 1 corresponds to no growth at all in
444 the presence of repressor. We used the area between the growth curves as opposed to growth rates,
445 because growth rates were hard to define under conditions with strong growth reductions: growth did
446 no longer show an exponential increase and the calculated rate was strongly dependent on the
447 specific time points used for determination. Furthermore, growth was generally slowing down over
448 time, and the repressor binding effects were not strictly limited to the 'exponential' growth phase.
449 Hence, a maximal growth rate would not capture all the effects and we chose to use a growth
450 measure that integrates over all of the growth phases and gives an impression of the general
451 decrease in fitness.

452

453 *DNA quantification*

454 The relative amount of DNA within the cells in rich and minimal media was determined using the
455 Wizard® Genomic DNA Purification Kit. We grew cells in LB or M9 with glucose to an OD of 0.2-0.3
456 and extracted genomic DNA using the purification kit. The amount of DNA was quantified by
457 nanodrop and normalized by OD, which gave a 2-fold higher amount of DNA in rich media than in
458 minimal media. This is an estimate of the minimal difference in DNA concentration as cells are slightly
459 bigger in LB than in M9- (Fig. S11).

460

461 *Protein quantification*

462 Repressor concentration was determined using the Promega Nano-Glo HiBit Lytic Detection System.
463 The HiBit peptide tag was attached at the N-terminal (which is involved in DNA binding) using a
464 (GGGS)₂ linker (sequence: GGTGGTGGTTCTGGTGGTGGTTCT) to assure accessibility of the tag
465 for interaction with the detection reagent. Briefly, cells induced (1ng or 25ng aTc) for expression of
466 wildtype repressor or repressor with the HiBit tag were grown to early exponential phase in minimal
467 media with glucose or rich media (LB), pelleted and frozen. Cells were resuspended in media and
468 supplemented with 0.1 culture volume of PopCulture Reagent (Sigma Aldrich), 10⁻³ culture volume
469 Benzonase Nuclease (Sigma Aldrich) and 0.5*10⁻³ culture volume lysozyme (Sigma Aldrich). Cells
470 were lysed for 30min at room temperature and then kept on ice. A protein standard (Promega) was
471 added to the non-tagged cells as a known reference of protein concentration to luminescence output.
472 Samples were mixed 1:1 with HiBit enzyme mixture and measured in white plates after shaking (in the
473 dark) for 15minutes. Dilution series of tagged repressor and protein standard were measured in a
474 Tecan platereader (Spark 10M) with an integration time of 1.5 seconds.
475 Repressor protein numbers in minimal media with glucose gave about 500 dimers per cell at 25ng
476 aTc and about 50 dimers per cell at 1ng aTc induction (as compared to ~125 dimers of λ CI in
477 lysogenic cells (27)). Similarly, we found around 500 dimers per cell at 25ng aTc in rich media. Note,
478 that the fitness reduction seen for λ CI concentrations at >1ng aTc induction (Fig. 2B) does not
479 directly translate to lysogenic cell fitness as it is masked by phage induction, superinfection and
480 superinfection exclusion (71) effects.

481

482 *Competition assays*

483 In order to distinguish between strains carrying a phage repressor (showing growth reduction) or the
484 bacterial repressor Lacl (not showing growth reduction), we used the pZS plasmid carrying *lacl* (under
485 the control of *P_{LtetO-1}*), together with a constitutively expressed fluorescence marker (*venus*) cloned in
486 the opposite direction upstream of *P_{LtetO-1}*. Venus was expressed from a mutated version of P_R, which
487 abolishes λ CI binding affinity in the *O_{R1}* operator (72,73) (the *O_{R1}* sequence used is:
488 TGCCTTAATACTGGATA) – and does not contain *O_{R2}* or *O_{R3}*- and is therefore constitutive
489 ('P_{constitutive}'). The fluorescence marker was placed on the Lacl-carrying plasmid because Lacl only had
490 a minor growth effect in *S. enterica* and none in *E. coli* (Fig. 4B, Table S5), which did not lead to
491 filamentation and hence did not affect fluorescence due to cell morphology changes. The lack of
492 growth reduction due to Lacl expression agrees with previous findings that GalR (and possibly other
493 members of the GalR family like Lacl) seem to have evolved to have fewer low-specificity sites across
494 the chromosome (18,29). There was only a slight fitness cost due to the presence of the fluorescence
495 marker on the plasmid (leading to a selection coefficient of 0.05 and 0.09 in *E. coli* and *S. enterica* for
496 the Lacl-carrying plasmid without the marker over the one with the marker), which however only
497 strengthens our findings that Lacl-expressing cells increase in competition with phage repressor-
498 expressing cells despite this cost.

499 A single colony for each host strain (*E. coli* or *S. enterica*) – plasmid (pZS21-*lacl*, pZS21- λ *ci*, pZS21-
500 *P22 c2*, pZS21- λ *ci* dimerization mutant, pZS21-*lacl*-P_{constitutive}-*venus*) combination was picked from a
501 freshly streaked plate and grown overnight in minimal media supplied with 0.2% glucose and 50 μ g/ml

502 kanamycin. Strains containing a phage repressor plasmid were mixed 1:1 with a strain carrying
503 pZS21-*lacI*-P_{constitutive}-*venus*, diluted 1:100 into fresh medium and grown in 96-wellplates for 10h.
504 Fluorescence was measured every 30min. and compared between cultures that were induced with
505 aTc (at concentrations as indicated, either 1, 2, 3, 4 or 25ng) and cultures that were not induced. This
506 means that we compared the abundance of fluorescent cells (i.e. abundance of *LacI*-carrying cells)
507 between cultures expressing and not expressing the repressor.
508 Selection coefficients were calculated using $\ln[(R^+_t/R^-_t)/(R^+_0/R^-_0)]$, where R^+_t and R^-_t represent
509 fluorescence measurements (as a proxy for relative *LacI*-expressing cell density) of cells with and
510 without inducer aTc (presence or absence of repressor expression) at time $t=10h$ respectively, and
511 R^+_0 and R^-_0 represent fluorescence measurements at the beginning of the experiment.

512

513 *Microscope fluorescence measurements*

514 A Nikon Ti-E microscope equipped with a thermostat chamber (TIZHB, Tokai Hit), 100x oil immersion
515 objective (Plan Apo λ , N.A. 1.45, Nikon), cooled CCD camera (ORCA-Flash, Hamamatsu Photonics)
516 and LED excitation light source (DC2100, Thorlabs) was used for the microscopy fluorescence
517 measurements of *PsuIA*-Yfp and *SeqA*-Gfp. The microscope was controlled by micromanager
518 (<https://micro-manager.org>). The cells were grown overnight in minimal media with glucose, diluted
519 1:100 in fresh media and grown to early exponential phase in the presence of the inducer aTc. YFP or
520 GFP fluorescence (where appropriate), RFP fluorescence (for image correction) and phase contrast
521 images were taken simultaneously at 3-min time-lapse intervals. Multiple patches of cells were
522 monitored in a single experiment. A custom macro of ImageJ (<http://imagej.nih.gov/ij/>) was used for
523 image analysis.

524 Imaging of cell membranes and DNA positioning was done using a Leica DMI6000B (inverted)
525 microscope with an Andor iXon EM CCD camera (front illuminated, 8x8 square micron pixel size) and
526 a 100x 1,47Na Oil HCX Plan Apo objective, giving an effective pixel size of 64nm/pixel. Images were
527 acquired using 405(20)nm and 561(10)nm laser excitation for blue (Hoechst) and red (NileRed) dyes
528 respectively. The cells were grown overnight in minimal media with glucose or LB, diluted 1:100 in
529 fresh media and grown to early exponential phase in the absence or presence of the inducer aTc.
530 After addition of both dyes (Hoechst at 10ug/mL and NileRed at 1ug/mL), cells were shaken at room
531 temperature for one hour and imaged in drops of the respective growth media. Images were
532 deconvolved using Huygens Professional (version 4.5) and further analyzed using ImageJ.

533

534 *ChIP-sequencing*

535 To perform ChIP-sequencing experiments, λ CI was cloned with an HA-Tag at the carboxy-terminal
536 end and transformed into both host strains. HA-tagged λ CI showed the same growth phenotype as
537 wildtype in both bacterial strains (Fig. S13). Samples from strains grown in the presence or absence
538 of λ CI were prepared according to Waldminghaus & Skarstad (2010)(74); library preparation and
539 Illumina Sequencing was performed at the VBCF NGS Unit (www.vbcf.ac.at). The obtained data was
540 analyzed using Galaxy and RStudio.

541 Peak calling was performed using custom R scripts modified from Santhanam et al. (75). Briefly, the
542 genome was computationally partitioned into non-overlapping shorter fragments, typically spanning a
543 few kbs to account for local biases arising from sequence content and immuno-precipitation (76,77).
544 Peak calling was performed within these fragments using partially overlapping (50% overlap) windows
545 of 100bp. For each window, we calculated strand-specific enrichment as the log-ratio of the scaled
546 read coverage between the sample and control ChIP-seq experiments while permitting a maximum of
547 5 reads to be mapped to the same genomic coordinates. We calculated strand-wise p-values for
548 enrichment by first resampling scaled read coverage within each fragment and then randomly
549 partitioning them to calculate enrichments. Finally, we identified bound regions to be those
550 with positive enrichment scores on both strands with a Benjamini-Hochberg false-discovery rate of
551 less than 30% as we were looking for binding of low specificity and ChIP-binding data was previously
552 found to be highly informative for a wide range of specificity profiles (78). For the regions that showed
553 significant enrichment in this analysis we plotted the read-depth across the genome in Fig. 5 (A,B)
554 and for comparison we plotted the read-depth for not significantly enriched regions in Fig. S4. As
555 control for our ChIP-sequencing procedure and analysis we used antibodies against SeqA, which
556 gave the expected peaks as published previously (74).
557 We calculated the nucleotide composition of the sequences underlying enriched regions in ChIP-seq
558 data for both bacterial species (Fig. S6). In order to test for sequence composition bias in these
559 enriched regions, we sought to test if the sequence compositions of the enriched regions were
560 significantly different compared to the rest of the genome. To this end, we randomly selected 50
561 genomic regions with at least 5kbp distance between them. We then calculated the nucleotide
562 composition of these randomly selected regions and by repeating this procedure 1000 times,
563 generated a null distribution for sequence composition of randomly selected genomic regions.
564 Similarly, we calculated the di-nucleotide composition (with 1 bp overlap) of the same randomly
565 selected genomic regions and compared it to that of the enriched regions.
566 The number of reads within 1000bp windows was compared with the predicted binding by calculating
567 binding energy at each genome position (using a sliding window approach) from the λ CI offset (i.e.
568 the energy difference between the repressor being bound specifically to an operator and being free in
569 solution (79)) and the energy penalty as given by the λ CI energy matrix (73). Smaller energies result
570 in stronger binding, meaning positive energy penalties decrease binding affinity (note that negative
571 penalties could increase binding over the one seen with λ CI wildtype operator sites). Binding strength
572 was calculated using $1/(1+\exp(E-\mu))$, with E being the calculated binding energy, as described above
573 and used in (24), and μ being the chemical potential, which we optimized to give the highest
574 Spearman correlation fit (2.6 in *E. coli* and 2 in *S. enterica*). For comparison with the number of ChIP-
575 sequencing reads, calculated binding strength was summed over the same genomic 1000bp regions
576 (considering binding to both strands). In Fig. 5 (C,D) we plot a non-parametric, non-linear relationship
577 estimate between the predicted binding energy and the ChIP-sequencing reads obtained from a
578 series of conditional medians. To investigate the dependence of the correlation between the affinity
579 predictions and the ChIP-sequencing reads on the structural versus the sequence information
580 contained in the energy matrix, we repeated the analysis with i) a matrix of the same size that

581 conserves only the ACGT bias of the λ CI energy matrix (each row contains the average value of that
582 row) or ii) matrices that had completely reshuffled entries. For the latter the average correlation was
583 taken over 100 permutations.

584 To assess the importance of specific sequence information versus nucleotide (GC) bias, we used a
585 Monte-Carlo permutation test: We calculated the difference between Spearman correlations of ChIP
586 reads with binding prediction using the wildtype energy matrix vs binding prediction using the energy
587 matrix that only conserves λ CI basepair bias, for the true ChIP read assignment, and 10^4 random
588 read assignments (null distribution). We found an overall strongly significant difference in *E. coli* and
589 lower significance in *S. enterica* (Fig. 5C,D), even though the effect size was small. This means that
590 while most of the measured ChIP signal can be accounted for by a TF model that predicts binding
591 based on the nucleotide content of genomic fragments alone, there is a small but highly significant
592 residual ChIP binding signal that requires the full binding site preference (energy matrix), not just
593 single nucleotide bias, to be explained. Further, we examined the influence of GC content by
594 repeating the Monte-Carlo permutation test for genomic sequences of a specific GC %. Here, we
595 found only a significant motif contribution for the 49% bin in *E. coli* (Fig. S7).

596 Additionally we used the offset and energy matrix for LacI (25,80) and P22 C2 (81) to predict binding
597 and calculate the Spearman correlation with the λ CI ChIP-sequencing reads (Fig. S5). Basepair bias
598 of the energy matrices was calculated as the sum of the average A and T preference minus the sum
599 of the average G and C preference.

600

601 *Statistical analysis*

602 Collected data was tested for normality (Shapiro-test) and subsequently we compared mean OD₆₀₀ or
603 fluorescence expression values using t-tests with FDR correction for multiple comparisons in RStudio.
604 T-tests were performed for four different time points between cultures grown in the presence and
605 absence of inducer aTc (presence or absence of repressors) under indicated conditions. Error bars on
606 growth reductions from AUC differences were obtained as 95% confidence intervals through
607 bootstrapping by resampling the data at each time point 1000 times.

608 Spearman correlation was calculated for the fit between model predictions of binding strength and the
609 number of obtained ChIP-sequencing reads per 1000bp window. P-values for WT and basepair bias
610 energy matrix predictions were $P < .001$ and for the average over random matrices $P < .01$.

611

612 **ACKNOWLEDGEMENT**

613 We thank T. Bergmiller, R. Chait, K. Jain, M. La Fortezza and the ETH Zurich ScopeM facility for their
614 support with fluorescence microscopy, B. Kavčič for his help with protein concentration
615 measurements, and T. Friedlander and J. Crocker for useful discussions. C.I. is the recipient of a
616 DOC Fellowship of the Austrian Academy of Sciences. Library preparation and sequencing of ChIP
617 seq samples was performed by the Next Generation Sequencing Facility at Vienna BioCenter Core
618 Facilities (VBCF), member of the Vienna BioCenter (VBC), Austria.

619

620 **AUTHOR CONTRIBUTIONS**

621 C.I., C.F., G.T. and C.C.G. conceived the study together. C.I. designed the experiments and carried
622 them out together with C.F. (growth experiments) and T.W. (ChIP-sequencing). C.I. analyzed the data
623 with input from F.M.P. and B.S.. C.I. wrote the initial draft of the manuscript and revised it together with
624 the rest of the authors.

625

626 **CONFLICT OF INTEREST**

627 Authors declare no competing financial interests.

628

629 **REFERENCES**

- 630 1. Hopfield JJ. Biosynthetic Processes Requiring High Specificity. *Pnas*. 1974;71(10):4135–9.
- 631 2. Mirny L, Slutsky M, Wunderlich Z, Tafvizi A, Leith J, Kosmrlj A. How a protein searches for its
632 site on DNA: the mechanism of facilitated diffusion. *J Phys A Math Theor* [Internet]. 2009 Oct
633 30;42(43):434013. Available from: [http://stacks.iop.org/1751-](http://stacks.iop.org/1751-8121/42/i=43/a=434013?key=crossref.c3b19cfa3ebb32a80370e612c091028f)
634 [8121/42/i=43/a=434013?key=crossref.c3b19cfa3ebb32a80370e612c091028f](http://stacks.iop.org/1751-8121/42/i=43/a=434013?key=crossref.c3b19cfa3ebb32a80370e612c091028f)
- 635 3. Elf J, Li G-W, Xie XS. Probing transcription factor dynamics at the single-molecule level in a
636 living cell. *Science* [Internet]. 2007 May 25;316(5828):1191–4. Available from:
637 <http://www.sciencemag.org/cgi/doi/10.1126/science.1141967>
- 638 4. Flyvbjerg H, Keatch SA, Dryden DTF. Strong physical constraints on sequence-specific target
639 location by proteins on DNA molecules. *Nucleic Acids Res*. 2006;34(9):2550–7.
- 640 5. von Hippel PH, Revzin A, Gross CA, Wang AC. Non-specific DNA binding of genome
641 regulating proteins as a biological control mechanism: I. The lac operon: equilibrium aspects.
642 *Proc Natl Acad Sci U S A*. 1974 Dec;71(12):4808–12.
- 643 6. Bakk A, Metzler R. Nonspecific binding of the OR repressors CI and Cro of bacteriophage
644 lambda. *J Theor Biol* [Internet]. 2004 Dec 21;231(4):525–33. Available from:
645 <https://linkinghub.elsevier.com/retrieve/pii/S0022519304003285>
- 646 7. Kao-Huang Y, Revzin A, Butler AP, O'Conner P, Noble DW, Von Hippel PH. Nonspecific DNA
647 binding of genome-regulating proteins as a biological control mechanism: measurement of
648 DNA-bound Escherichia coli lac repressor in vivo. *Proc Natl Acad Sci U S A* [Internet].
649 1977;74(10):4228–32. Available from:
650 <http://www.pnas.org/content/74/10/4228.short%5Cnhttp://www.pubmedcentral.nih.gov/articlerender.fcgi?artid=431912&tool=pmcentrez&rendertype=abstract>
- 651 8. Gerland U, Moroz JD, Hwa T. Physical constraints and functional characteristics of
652 transcription factor-DNA interaction. *Proc Natl Acad Sci U S A*. 2002;99(19):12015–20.
- 653 9. Spurio R, Dürrenberger M, Falconi M, La Teana A, Pon CL, Gualerzi CO. Lethal
654 overproduction of the Escherichia coli nucleoid protein H-NS: ultramicroscopic and molecular
655 autopsy. *MGG Mol Gen Genet*. 1992;231(2):201–11.
- 656 10. Yamada H, Yoshida T, Tanaka K ichi, Sasakawa C, Mizuno T. Molecular analysis of the
657 Escherichia coli has gene encoding a DNA-binding protein, which preferentially recognizes
658 curved DNA sequences. *MGG Mol Gen Genet*. 1991;230(1–2):332–6.
- 659 11. Crocker J, Preger-Ben Noon E, Stern DL. The Soft Touch. In: *Current Topics in*
660 *Developmental Biology* [Internet]. 1st ed. Elsevier Inc.; 2016. p. 455–69. Available from:
661 <http://dx.doi.org/10.1016/bs.ctdb.2015.11.018>
- 662 12. Burger A, Walczak AM, Wolynes PG. Abduction and asylum in the lives of transcription
663 factors. *Proc Natl Acad Sci* [Internet]. 2010;107(9):4016–21. Available from:
664 <http://www.pnas.org/cgi/doi/10.1073/pnas.0915138107>
- 665 13. Friedlander T, Prizak R, Guet C, Barton NH. Intrinsic limits to gene regulation by global
666 crosstalk. 2015;
- 667 14. Cepeda-Humerez SA, Rieckh G, Tkačik G. Stochastic Proofreading Mechanism Alleviates
668 Crosstalk in Transcriptional Regulation. *Phys Rev Lett*. 2015;115(24):1–5.
- 669 15. Grah R, Zoller B, Tkačik G. Nonequilibrium models of optimal enhancer function. *Proc Natl*
670 *Acad Sci U S A*. 2020;117(50):31614–22.
- 671 16. Sasson V, Shachrai I, Bren A, Dekel E, Alon U. Mode of Regulation and the Insulation of
672 Bacterial Gene Expression. *Mol Cell* [Internet]. 2012;46(4):399–407. Available from:
673 <http://dx.doi.org/10.1016/j.molcel.2012.04.032>
- 674 17. Howard-Varona C, Hargreaves KR, Abedon ST, Sullivan MB. Lysogeny in nature:
675 mechanisms, impact and ecology of temperate phages. *ISME J* [Internet]. 2017 Jul
676

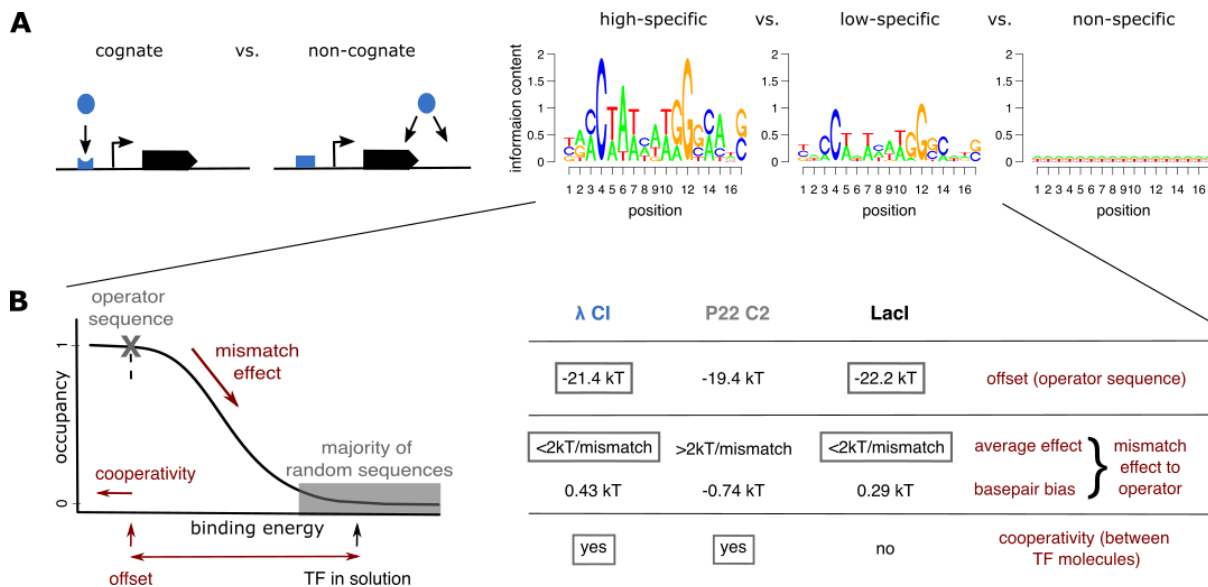
- 677 14;11(7):1511–20. Available from: <http://dx.doi.org/10.1038/ismej.2017.16>
- 678 18. Shimada T, Ogasawara H, Ishihama A. Single-target regulators form a minor group of
679 transcription factors in *Escherichia coli* K-12. *Nucleic Acids Res.* 2018;46(8):3921–36.
- 680 19. Ptashne M. Principles of a switch. *Nat Chem Biol* [Internet]. 2011 Aug [cited 2014 Jun
681 3];7(8):484–7. Available from: <http://www.ncbi.nlm.nih.gov/pubmed/21769089>
- 682 20. Priest DG, Cui L, Kumar S, Dunlap DD, Dodd IB, Shearwin KE. Quantitation of the DNA
683 tethering effect in long-range DNA looping in vivo and in vitro using the Lac and repressors.
684 *Proc Natl Acad Sci* [Internet]. 2014;111(1):349–54. Available from:
685 <http://www.pnas.org/cgi/doi/10.1073/pnas.1317817111>
- 686 21. Donner AL, Carlson PA, Koudelka GB. Dimerization specificity of P22 and 434 repressors is
687 determined by multiple polypeptide segments. *J Bacteriol* [Internet]. 1997 Feb [cited 2014 Jul
688 8];179(4):1253–61. Available from:
689 <http://www.pubmedcentral.nih.gov/articlerender.fcgi?artid=178823&tool=pmcentrez&rendertype=abstract>
- 690
- 691 22. Pray TR, Burz DS, Ackers GK. Cooperative non-specific DNA binding by octamerizing λ CI
692 repressors: a site-specific thermodynamic analysis. *J Mol Biol* [Internet]. 1998 Oct [cited 2017
693 Mar 1];282(5):947–58. Available from:
694 <https://linkinghub.elsevier.com/retrieve/pii/S0022283698920563>
- 695 23. Bakk A, Metzler R. In vivo non-specific binding of λ CI and Cro repressors is significant. *FEBS*
696 *Lett.* 2004;563(1–3):66–8.
- 697 24. Iglér C, Lagator M, Tkačik G, Bollback JP, Guet CC. Evolutionary potential of transcription
698 factors for gene regulatory rewiring. *Nat Ecol Evol.* 2018;2(October).
- 699 25. Vilar JM, Saiz L. DNA looping in gene regulation: from the assembly of macromolecular
700 complexes to the control of transcriptional noise. *Curr Opin Genet Dev* [Internet]. 2005 Apr
701 [cited 2014 May 14];15(2):136–44. Available from:
702 <http://www.ncbi.nlm.nih.gov/pubmed/15797196>
- 703 26. Fattah KR, Mizutani S, Fattah FJ, Matsushiro A, Sugino Y. A comparative study of the
704 immunity region of lambdoid phages including Shiga-toxin-converting phages : molecular basis
705 for cross immunity . 2000;223–32.
- 706 27. Oppenheim AB, Kobilier O, Stavans J, Court DL, Adhya S. Switches in bacteriophage lambda
707 development. *Annu Rev Genet* [Internet]. 2005 Jan [cited 2014 May 24];39:409–29. Available
708 from: <http://www.ncbi.nlm.nih.gov/pubmed/16285866>
- 709 28. Schlechter RO, Remus DM, Remus-Emsermann MNP. Constitutively expressed fluorescent
710 proteins allow to track bacterial growth and to determine relative fitness of bacteria in mixed
711 cultures. *bioRxiv.* 2020;(Figure 1):1–5.
- 712 29. Chakrabarti J, Chandra N, Raha P, Roy S. High-affinity quasi-specific sites in the genome:
713 How the DNA-binding proteins cope with them. *Biophys J* [Internet]. 2011;101(5):1123–9.
714 Available from: <http://dx.doi.org/10.1016/j.bpj.2011.07.041>
- 715 30. Whipple FW, Kuldell NH, Cheatham LA, Hochschild A. Specificity determinants for the
716 interaction of lambda repressor and P22 repressor dimers. *Genes Dev* [Internet]. 1994 May 15
717 [cited 2014 Sep 22];8(10):1212–23. Available from:
718 <http://www.genesdev.org/cgi/doi/10.1101/gad.8.10.1212>
- 719 31. Weiss MA, Pabo CO, Karplus M, Sauer RT. Dimerization of the operator binding domain of
720 phage lambda repressor. *Biochemistry* [Internet]. 1987 Feb 10 [cited 2014 Jun 5];26(3):897–
721 904. Available from: <http://dx.doi.org/10.1021/bi00377a034>
- 722 32. Nelson HCM, Sauer RT. Interaction of mutant λ repressors with operator and non-operator
723 DNA. *J Mol Biol.* 1986;192(1):27–38.
- 724 33. Mazumder A, Batabyal S, Mondal M, Mondol T, Choudhury S, Ghosh R, et al. Specific DNA
725 sequences allosterically enhance protein-protein interaction in a transcription factor through
726 modulation of protein dynamics: Implications for specificity of gene regulation. *Phys Chem*
727 *Chem Phys* [Internet]. 2017;19(22):14781–92. Available from:
728 <http://dx.doi.org/10.1039/C7CP01193H>
- 729 34. Guarnaccia C, Raman B, Zahariev S, Simoncsits A, Pongor S. DNA-mediated assembly of
730 weakly interacting DNA-binding protein subunits: In vitro recruitment of phage 434 repressor
731 and yeast GCN4 DNA-binding domains. *Nucleic Acids Res.* 2004;32(17):4992–5002.
- 732 35. Maerkl SJ, Quake SR. A Systems Approach to Measuring the Binding Energy Landscapes of
733 Transcription Factors. *Science (80-)* [Internet]. 2007 Jan 12;315(5809):233–7. Available from:
734 <http://www.ncbi.nlm.nih.gov/pubmed/17218526>
- 735 36. Sarkar-Banerjee S, Goyal S, Gao N, Mack J, Thompson B, Dunlap D, et al. Specifically bound
736 lambda repressor dimers promote adjacent non-specific binding. Saiz L, editor. *PLoS One*

- 737 [Internet]. 2018 Apr 2;13(4):e0194930. Available from:
738 <http://dx.doi.org/10.1371/journal.pone.0194930>
- 739 37. Chen Y, Golding I, Sawai S, Guo L, Cox EC. Population Fitness and the Regulation of
740 *Escherichia coli* Genes by Bacterial Viruses. Waldor M, editor. PLoS Biol [Internet]. 2005 Jun
741 21;3(7):e229. Available from: <http://dx.plos.org/10.1371/journal.pbio.0030229>
- 742 38. Nordström K, Dasgupta S. Copy-number control of the *Escherichia coli* chromosome: A
743 plasmidologist's view. EMBO Rep. 2006;7(5):484–9.
- 744 39. Cooper S, Ruettinger T. Replication of deoxyribonucleic acid during the division cycle of
745 *Salmonella typhimurium*. J Bacteriol. 1973;114(3):966–73.
- 746 40. Klumpp S, Zhang Z, Hwa T. Growth Rate-Dependent Global Effects on Gene Expression in
747 Bacteria. Cell [Internet]. 2009 Dec;139(7):1366–75. Available from:
748 <http://dx.doi.org/10.1016/j.cell.2009.12.001>
- 749 41. Deris JB, Kim M, Zhang Z, Okano H, Hermsen R, Groisman A, et al. The Innate Growth
750 Bistability and Fitness Landscapes of Antibiotic-Resistant Bacteria. Science (80-) [Internet].
751 2013 Nov 29;342(6162):1237435–1237435. Available from:
752 <http://www.sciencemag.org/cgi/doi/10.1126/science.1237435>
- 753 42. Waldminghaus T, Weigel C, Skarstad K. Replication fork movement and methylation govern
754 SeqA binding to the *Escherichia coli* chromosome. Nucleic Acids Res. 2012;40(12):5465–76.
- 755 43. Sauer RT, Ross MJ, Ptashne M. Cleavage of the lambda and P22 repressors by recA protein.
756 J Biol Chem. 1982 Apr;257(8):4458–62.
- 757 44. Phizicky EM, Roberts JW. Kinetics of recA protein-directed inactivation of repressors of phage
758 lambda and phage P22. J Mol Biol. 1980;139(3):319–28.
- 759 45. Arends SJR, Weiss DS. Inhibiting Cell Division in *Escherichia coli* Has Little If Any Effect on
760 Gene Expression. J Bacteriol [Internet]. 2004 Feb 1;186(3):880–4. Available from:
761 <http://jb.asm.org/cgi/doi/10.1128/JB.186.3.880-884.2004>
- 762 46. Cambridge J, Blinkova A, Magnan D, Bates D, Walker JR. A Replication-inhibited
763 unsegregated nucleoid at mid-cell blocks Z-ring formation and cell division independently of
764 SOS and the SlmA nucleoid occlusion protein in *Escherichia coli*. J Bacteriol. 2014;196(1):36–
765 49.
- 766 47. Gullbrand B, Nordström K. FtsZ ring formation without subsequent cell division after replication
767 runout in *Escherichia coli*. Mol Microbiol [Internet]. 2002 Jan 18;36(6):1349–59. Available from:
768 <http://doi.wiley.com/10.1046/j.1365-2958.2000.01949.x>
- 769 48. Wunderlich Z, Mirny L. Fundamentally different strategies for transcriptional regulation are
770 revealed by analysis of binding motifs. Nat Preced. 2008;2(i).
- 771 49. Brewster RC, Weinert FM, Garcia HG, Song D, Rydenfelt M, Phillips R. The transcription
772 factor titration effect dictates level of gene expression. Cell. 2014;156(6):1312–23.
- 773 50. Pleška M, Qian L, Okura R, Bergmiller T, Wakamoto Y, Kussell E, et al. Bacterial
774 Autoimmunity Due to a Restriction-Modification System. Curr Biol [Internet]. 2016 Feb
775 8;26(3):404–9. Available from: <http://www.ncbi.nlm.nih.gov/pubmed/26804559>
- 776 51. de Boer PAJ. Advances in understanding *E. coli* cell fission. Curr Opin Microbiol.
777 2010;13(6):730–7.
- 778 52. Sun Q, Margolin W. Effects of perturbing nucleoid structure on nucleoid occlusion-mediated
779 toporegulation of FtsZ ring assembly. J Bacteriol. 2004;186(12):3951–9.
- 780 53. Spurio R, Falconi M, Brandi A, Pon CL, Gualerzi CO. The oligomeric structure of nucleoid
781 protein H-NS is necessary for recognition of intrinsically curved DNA and for DNA bending.
782 EMBO J. 1997;16(7):1795–805.
- 783 54. Verma SC, Qian Z, Adhya SL. Architecture of the *Escherichia coli* nucleoid. Vol. 15, PLoS
784 Genetics. 2019. 1–35 p.
- 785 55. Amir A, Männik J, Woldringh CL, Zaritsky A. Editorial: The Bacterial Cell: Coupling between
786 Growth, Nucleoid Replication, Cell Division, and Shape Volume 2. Front Microbiol.
787 2019;10(September):1–3.
- 788 56. Zabet NR, Adryan B. The effects of transcription factor competition on gene regulation. Front
789 Genet. 2013;4(OCT):1–10.
- 790 57. Baltrus DA. Exploring the costs of horizontal gene transfer. Trends Ecol Evol [Internet].
791 2013;28(8):489–95. Available from: <http://dx.doi.org/10.1016/j.tree.2013.04.002>
- 792 58. Friedlander T, Prizak R, Barton NH, Tkačik G. Evolution of new regulatory functions on
793 biophysically realistic fitness landscapes. Nat Commun. 2017;8(1).
- 794 59. Lutz R, Bujard H. Independent and tight regulation of transcriptional units in *Escherichia coli*
795 via the LacR/O, the TetR/O and AraC/I1-I2 regulatory elements. Nucleic Acids Res [Internet].
796 1997 Mar 15;25(6):1203–10. Available from:

- 797 <http://www.pubmedcentral.nih.gov/articlerender.fcgi?artid=146584&tool=pmcentrez&rendertype=abstract>
798 e=abstract
- 799 60. Datsenko K a, Wanner BL. One-step inactivation of chromosomal genes in *Escherichia coli* K-
800 12 using PCR products. *Proc Natl Acad Sci U S A* [Internet]. 2000 Jun 6;97(12):6640–5.
801 Available from:
802 <http://www.pubmedcentral.nih.gov/articlerender.fcgi?artid=18686&tool=pmcentrez&rendertype=abstract>
803 =abstract
- 804 61. Kües U, Stahl U. Replication of plasmids in gram-negative bacteria. *Microbiol Rev* [Internet].
805 1989 Dec;53(4):491–516. Available from: <http://www.ncbi.nlm.nih.gov/pubmed/2687680>
- 806 62. Hershfield V, Boyer HW, Yanofsky C, Lovett MA, Helinski DR. Plasmid ColEI as a molecular
807 vehicle for cloning and amplification of DNA. *Proc Natl Acad Sci U S A*. 1974;71(9):3455–9.
- 808 63. Nagai T, Ibata K, Park ES, Kubota M, Mikoshiba K, Miyawaki A. A variant of yellow fluorescent
809 protein with fast and efficient maturation for cell-biological applications. *Nat Biotechnol*
810 [Internet]. 2002 Jan;20(1):87–90. Available from:
811 <http://www.ncbi.nlm.nih.gov/pubmed/11753368>
- 812 64. Nishihara K, Kanemori M, Yanagi H, Yura T. Overexpression of trigger factor prevents
813 aggregation of recombinant proteins in *Escherichia coli*. *Appl Environ Microbiol* [Internet]. 2000
814 Mar;66(3):884–9. Available from: <http://www.ncbi.nlm.nih.gov/pubmed/10698746>
- 815 65. Kitagawa M, Ara T, Arifuzzaman M, Ioka-Nakamichi T, Inamoto E, Toyonaga H, et al.
816 Complete set of ORF clones of *Escherichia coli* ASKA library (A complete set of *E. coli* K-12
817 ORF archive): unique resources for biological research. *DNA Res*. 2005;12(5):291–9.
- 818 66. Costantino N, Court DL. Enhanced levels of lambda Red-mediated recombinants in mismatch
819 repair mutants. *Proc Natl Acad Sci U S A* [Internet]. 2003;100(26):15748–53. Available from:
820 <http://www.pubmedcentral.nih.gov/articlerender.fcgi?artid=307639&tool=pmcentrez&rendertype=abstract>
821 e=abstract
- 822 67. Friedberg EC, Walker GC, Siede W, Wood RD. DNA repair and mutagenesis. American
823 Society for Microbiology Press; 2005.
- 824 68. Haldimann A, Wanner BL. Conditional-Replication, Integration, Excision, and Retrieval
825 Plasmid-Host Systems for Gene Structure-Function Studies of Bacteria. *J Bacteriol* [Internet].
826 2001 Nov 1;183(21):6384–93. Available from:
827 <http://jb.asm.org/cgi/doi/10.1128/JB.183.21.6384-6393.2001>
- 828 69. Marchetti A, Abril-Marti M, Illi B, Cesareni G, Nasi S. Analysis of the Myc and Max interaction
829 specificity with λ repressor-HLH domain fusions. *J Mol Biol*. 1995;248(3):541–50.
- 830 70. Wharton RP, Ptashne M. Changing the binding specificity of a repressor by redesigning an α -
831 helix. *Nature*. 1985;316(6029):601–5.
- 832 71. Lin L, Bitner R, Edlin G. Increased reproductive fitness of *Escherichia coli* lambda lysogens. *J*
833 *Virology*. 1977;21(2):554–9.
- 834 72. Flashman SM. NMutational Analysis of the Operators of Bacteriophage Lambda. 1978;73:61–
835 73.
- 836 73. Sarai A, Takeda Y. Lambda repressor recognizes the approximately 2-fold symmetric half-
837 operator sequences asymmetrically. *Proc Natl Acad Sci U S A* [Internet]. 1989;86(17):6513–7.
838 Available from:
839 <http://www.pubmedcentral.nih.gov/articlerender.fcgi?artid=297874&tool=pmcentrez&rendertype=abstract>
840 e=abstract
- 841 74. Waldminghaus T, Skarstad K. ChIP on Chip: surprising results are often artifacts. *BMC*
842 *Genomics* [Internet]. 2010;11(1):414. Available from: <http://www.biomedcentral.com/1471-2164/11/414>
843 2164/11/414
- 844 75. Santhanam B, Cai H, Devreotes PN, Shauly G, Katoh-Kurasawa M. The GATA transcription
845 factor GtaC regulates early developmental gene expression dynamics in *Dictyostelium*. *Nat*
846 *Commun*. 2015;6(May).
- 847 76. Jothi R, Cuddapah S, Barski A, Cui K, Zhao K. Genome-wide identification of in vivo protein-
848 DNA binding sites from ChIP-Seq data. *Nucleic Acids Res*. 2008;36(16):5221–31.
- 849 77. Zhang Y, Liu T, Meyer CA, Eeckhoutte J, Johnson DS, Bernstein BE, et al. Model-based
850 analysis of ChIP-Seq (MACS). *Genome Biol*. 2008;9(9).
- 851 78. Tanay A. Extensive low-affinity transcriptional interactions in the yeast genome. *Genome Res*
852 [Internet]. 2006 Jun 29;16(8):962–72. Available from:
853 <http://www.genome.org/cgi/doi/10.1101/gr.5113606>
- 854 79. Koblan KS, Ackers GK. Site-Specific Enthalpic Regulation of DNA Transcription at
855 Bacteriophage λ OR. *Biochemistry*. 1992;31(1):57–65.
- 856 80. Barne SL, Belliveau NM, Ireland WT, Kinney JB, Phillips R. Mapping DNA sequence to

857 transcription factor binding energy in vivo. PLoS Comput Biol. 2019;15(2):1–29.
858 81. Hilchey SP, Wu L, Koudelka GB. Recognition of Nonconserved Bases in the P22 Operator by
859 P22 Repressor Requires Specific Interactions between Repressor and Conserved Bases *.
860 1997;272(32):19898–905.
861
862

863 **FIGURE LEGENDS**



864

865 **Box 1. (A)** In order to elicit an appropriate function, TFs have to recognize their cognate DNA sites

866 (operators) among a large background of non-cognate sites, where binding is non-functional and

867 potentially interferes with cellular programs. Binding of TFs to cognate or non-cognate sites can occur

868 by recognizing a specific motif on the DNA (with specificity ranging from high to low, depending on the

869 overlap of the target site with the TF's consensus sequence (8)) or through generic, non-specific

870 interactions with any DNA sequence. **(B)** Binding with high specificity usually occurs to a TF-specific

871 DNA consensus motif and the offset gives the binding energy (lower energy = stronger binding) to a

872 single operator sequence relative to the unbound state (TF in solution). Random DNA sequences are

873 usually located at the lower end of the sigmoid (gray box) with energy values similar to that of the TF

874 in solution. Basepair mismatches with the operator sequence incur an energy penalty and increase

875 the binding energy (i.e. weaken the binding) based on two features: specific effects of basepair

876 mismatches and overall basepair bias (given here as average AT preference – average GC

877 preference). Hence, for a TF with low offset, which is aided by high cooperativity, and an energy

878 matrix characterized by small mismatch effects, many random sequences will not be far from the rise

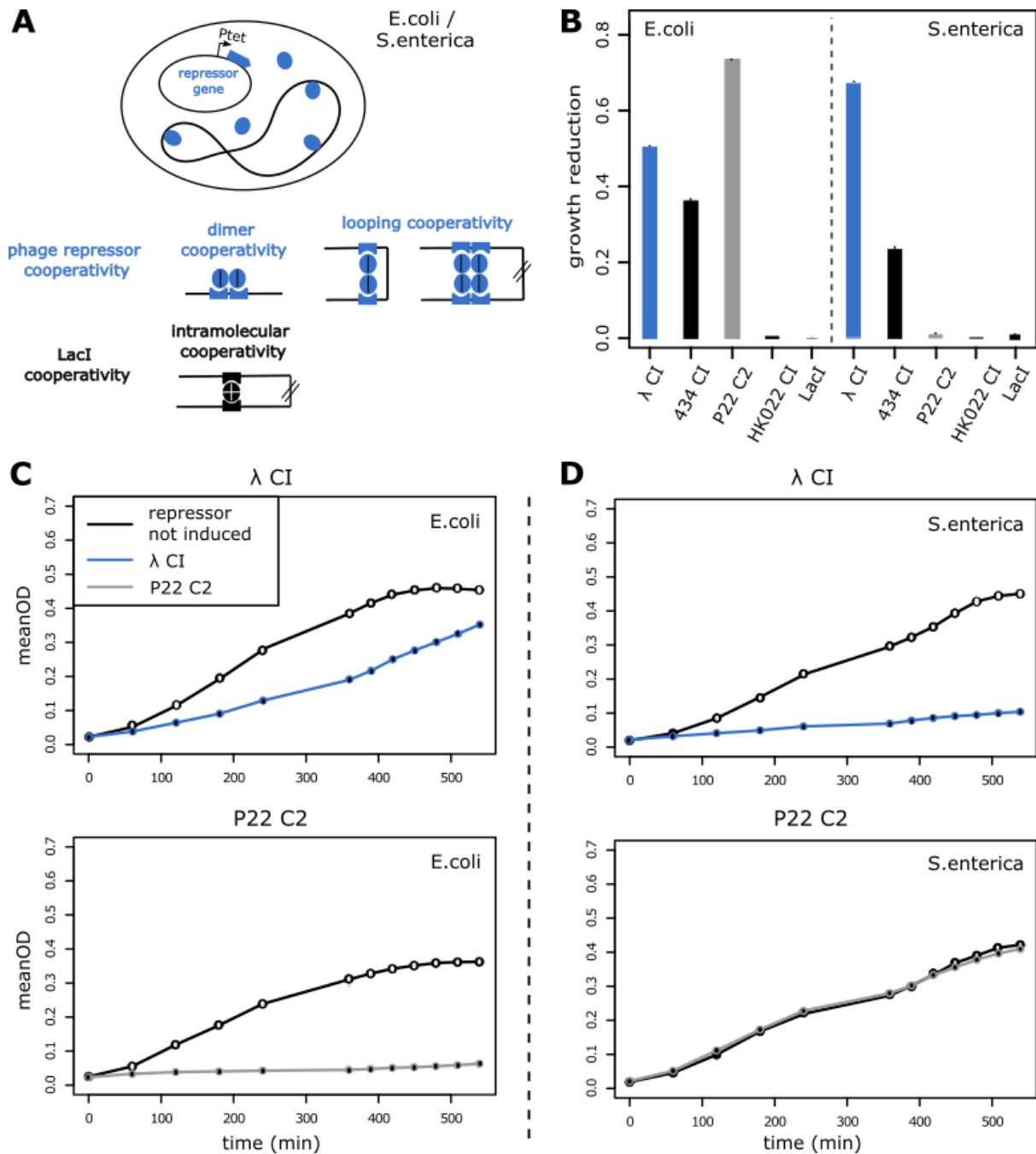
879 of the sigmoid, making higher occupancy at low specificity binding sites more likely. The table

880 compares these three criteria for three well-characterized TFs, showing that all of them are fulfilled for

881 λ CI, but only partially for P22 C2 and Lacl (24,25,80,81), making λ CI an obvious candidate for

882 substantial low-specificity non-cognate binding.

883



884

885 **Figure 1. Growth reduction in the presence of repressors in minimal media with glucose.**

886 **(A)** The experimental model system with repressors being expressed from a plasmid and their binding

887 cooperativity modes are shown. **(B)** Growth reduction as calculated by the normalized growth

888 difference in the presence and absence of repressor are shown for λ CI, 434 CI, P22 C2, HK022 CI

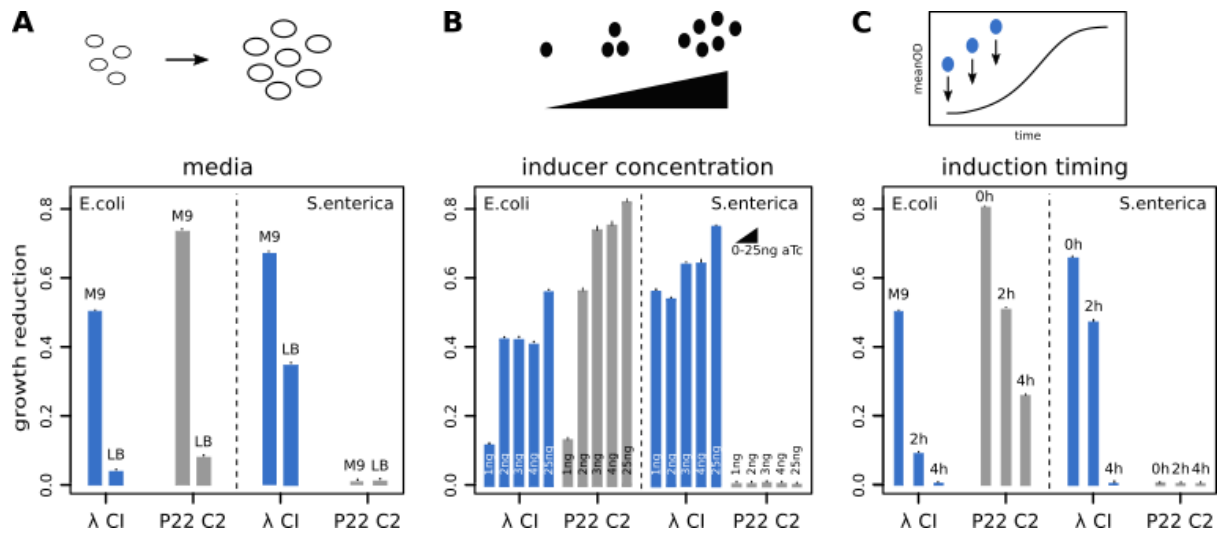
889 and LacI in *E. coli* and *S. enterica* cells. Error bars show 95% confidence intervals. **(C,D)** Curves

890 show mean OD₆₀₀ for *E. coli* (left) or *S. enterica* (right) cells in the presence (color) or absence (black)

891 of **(C)** λ CI or **(D)** P22 C2; error bars show standard deviation over 6 replicates (black on color and

892 white on black).

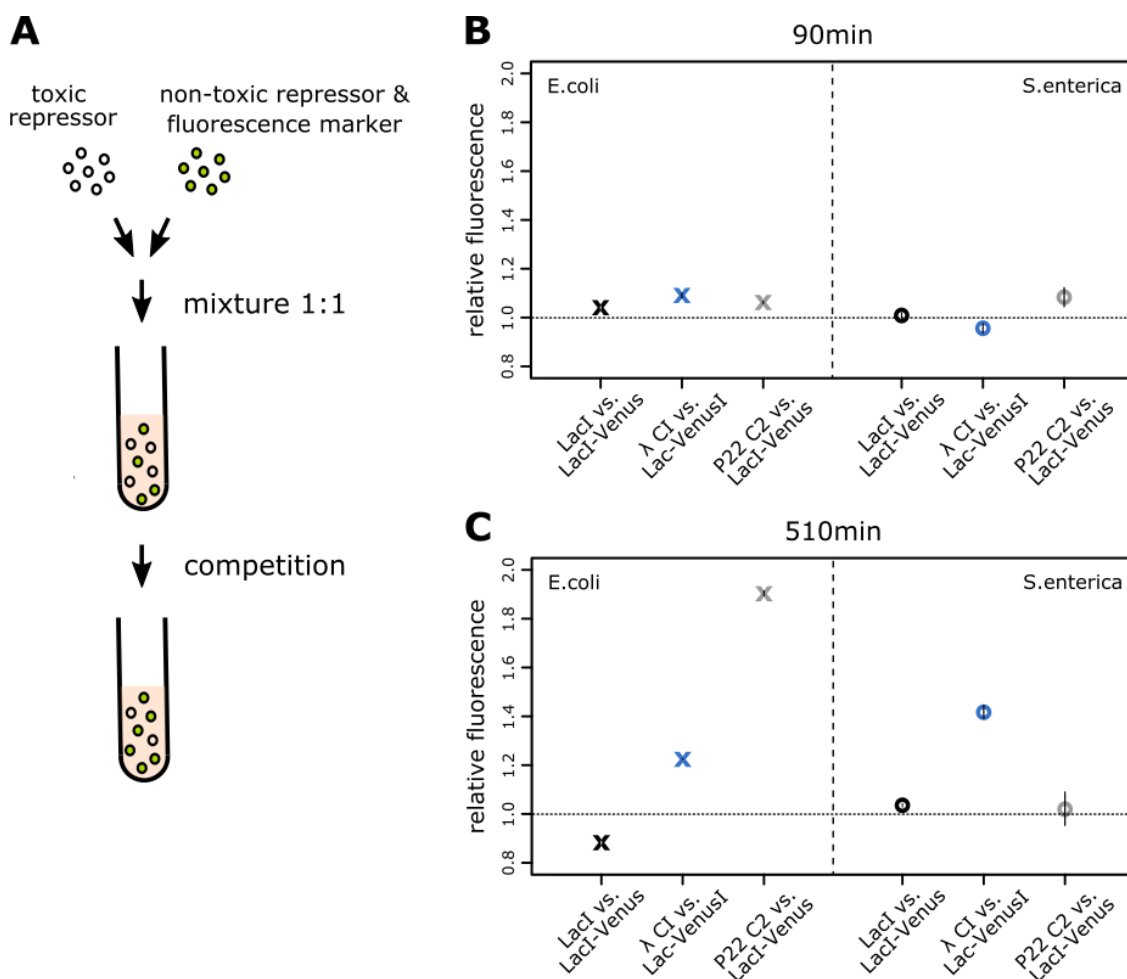
893



894

895 **Figure 2. Effect of environment on repressor-dependent growth reduction.**

896 Growth reduction as calculated by the normalized growth difference in the presence and absence of
 897 repressor are shown for λ CI (blue) and P22 C2 (grey) in *E. coli* and *S. enterica*. Error bars show 95%
 898 confidence intervals. **(A)** Cells were grown in minimal medium with glucose (M9) or rich media (LB) at
 899 full induction of repressors. **(B)** Inducer concentrations for repressor expression were varied from 1 to
 900 25ng (very low to full induction (59)). **(C)** Induction time points of repressor expression were varied
 901 from lag phase (0h) to early- (2h) and mid- exponential phase (4h).
 902



903

904

Figure 3. Competition assays reveal fitness cost of repressor expression.

905

(A) Cells containing plasmids with a repressor affecting growth (λ CI or P22 C2) or with a repressor not affecting growth (LacI) were mixed 1:1 with cells containing a plasmid with the repressor not affecting growth and a separately, constitutively expressed Venus marker (LacI-Venus). Competition was performed in minimal media with glucose and fluorescence was used as a measure of the

909

relative change in the cells carrying LacI-Venus. **(B,C)** Relative fluorescence was calculated for *E. coli*

910

(crosses) or *S. enterica* (circles) between induced and non-induced samples of cell mixtures of LacI-

911

Venus together with LacI (control), λ CI or P22 C2 after **(B)** 90min or **(C)** 510min of competition; error

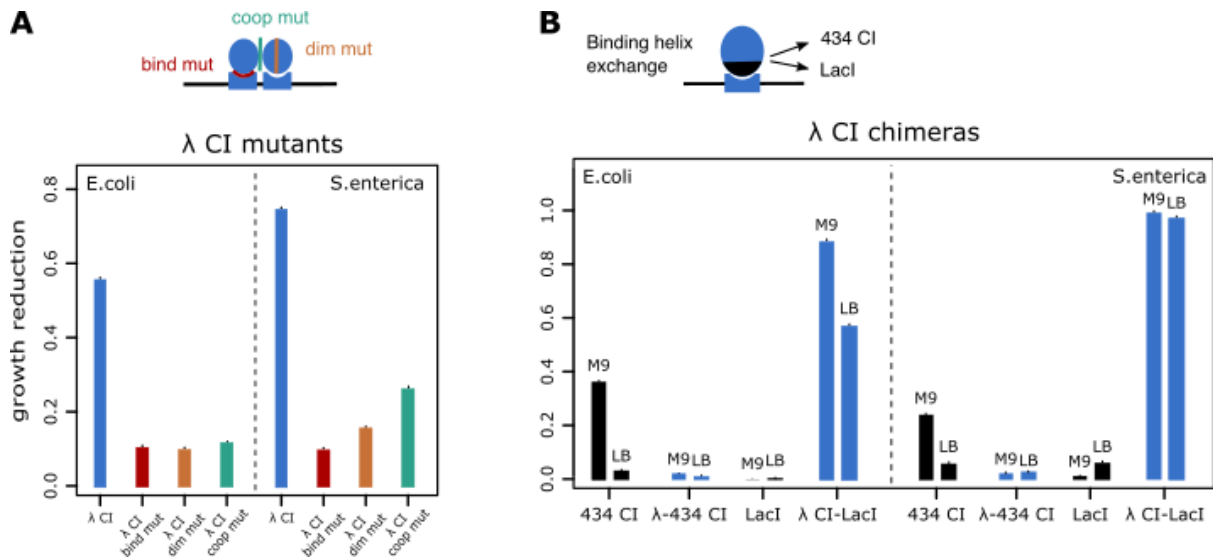
912

bars show relative errors. Selection coefficients (for calculation see Methods) after 10h were 0.27 (*E.*

913

coli) and 0.29 (*S. enterica*) for λ CI and 0.67 (*E. coli*) and -0.06 (*S. enterica*) for P22 C2.

914

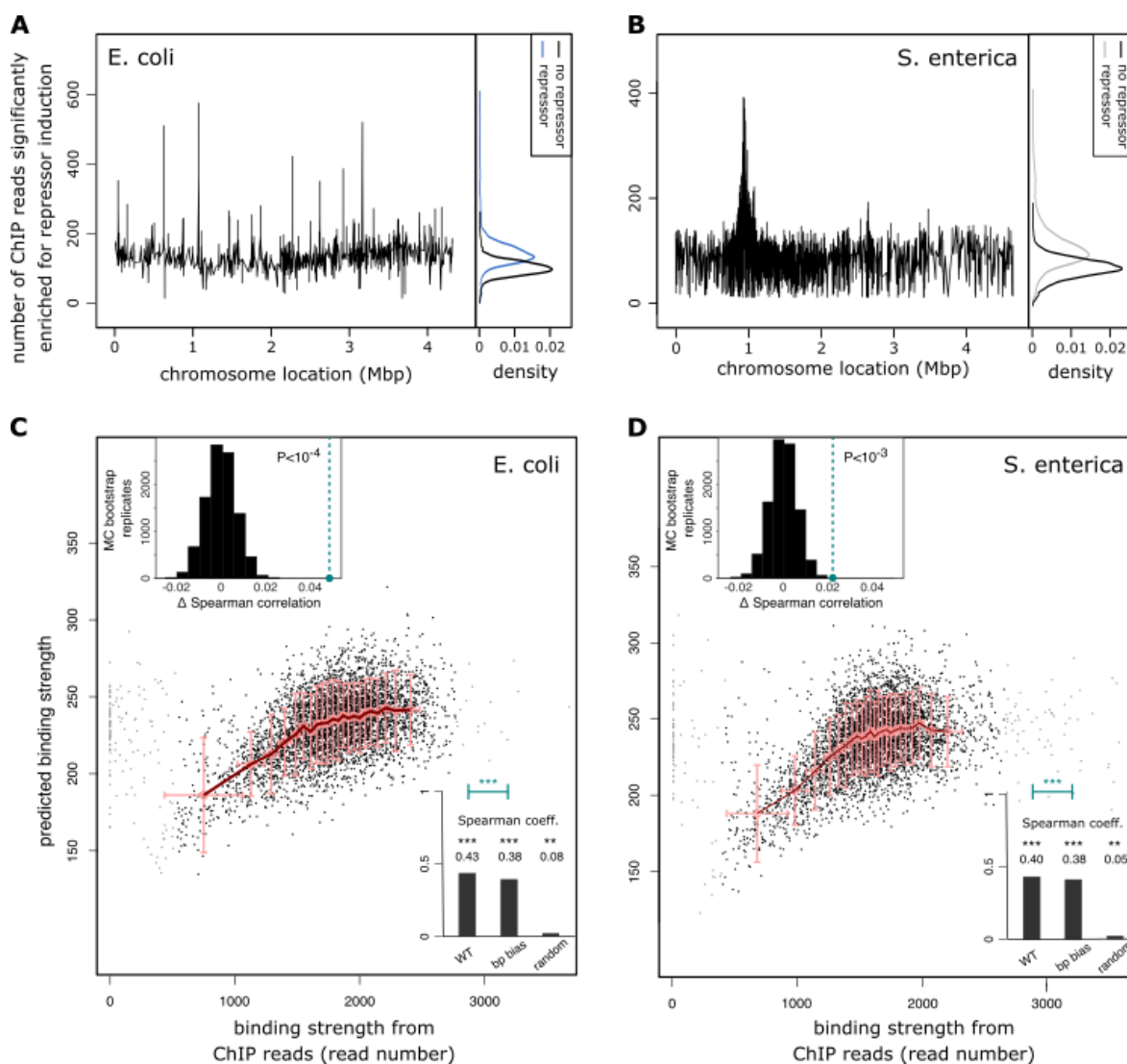


915

916 **Figure 4. Effect of mutants and chimeric proteins on repressor-dependent growth reduction.**

917 Growth reduction as calculated by the normalized growth difference in the presence and absence of
 918 repressor are shown in *E. coli* and *S. enterica*. Error bars show 95% confidence intervals. **(A)** Growth
 919 reduction for *λ* CI wildtype (blue) is compared to a *λ* CI binding mutant (red), a *λ* CI dimerization
 920 mutant (orange) or a *λ* CI cooperativity mutant (turquoise) in minimal media. **(B)** Growth reduction of
 921 the phage repressor 434 CI and the bacterial repressor LacI (black) compared to a chimera of the *λ*
 922 CI protein containing the binding specificity of either 434 CI (*λ*-434 CI) or LacI (*λ* CI-LacI) (blue) is
 923 shown for minimal (M9) and rich media (LB).

924



925

926 **Figure 5. Distributed, low-specificity binding of λ CI across the genomes of *E. coli* and *S.***

927 ***enterica*.**

928 **(A,B)** Distributions of ChIP-sequencing reads for the regions found to be significantly enriched in the
 929 experiment with λ CI over the experiment without λ CI across the **(A)** *E. coli* or **(B)** *S. enterica* genome.

930 On the right density plots of enriched read numbers are given for repressor (color) or no repressor
 931 (black) experiments (Number of reads for not significantly enriched regions are shown in Fig. S4 for
 932 comparison). None of the apparent peaks in **(A)** or **(B)** encodes for an essential gene, nor one obviously

933 beneficial in minimal media. **(C,D)** Fit between binding strength predictions of a simple thermodynamic
 934 model using the energy matrix for λ CI binding and the ChIP-sequencing reads across 1000bp windows

935 along the **(C)** *E. coli* or **(D)** *S. enterica* genome. In **(D)**, 33 out of 4856 data points showed more than
 936 3600 reads and were omitted for clarity (the data is available on request). Lower insets show the

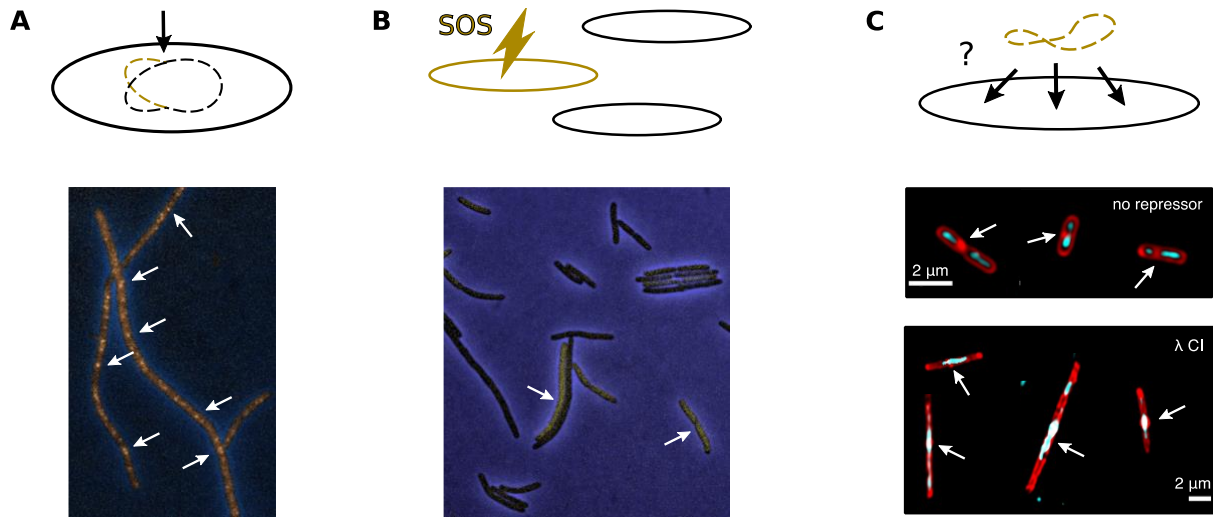
937 calculated Spearman correlations using either the wildtype energy matrix, one that only conserves the
 938 λ CI basepair bias (Fits are shown in Fig. S5) or one that has completely reshuffled entries (averaged

939 over 100 permutations). Upper insets: Permutation test for the significance of the difference in
 940 Spearman correlation between binding predictions using the wildtype energy matrix (first bar in the

941 lower inset) vs prediction with the energy matrix that only conserves λ CI basepair bias (second bar in

942 the lower inset). Black histograms represent the Monte-Carlo-derived null distribution (10^4 random
943 reassignments of ChIP reads to genomic regions), green dot and line show the true excess Spearman
944 correlation. The correlations for *S. enterica* were not substantially affected by the strong binding peak
945 in prophage regions shown in **(B)**.

946
947



948

949 **Figure 6. Induction of λ CI interferes with cell division but not DNA replication.**

950 Cells were imaged under the microscope in minimal media with glucose and aTc, either **(A,B)** on an
951 agar pad, or directly **(C)** in liquid media (see Methods). Fluorescence indicates **(A)** ongoing replication
952 (a SeqA-GFP fusion as a replication fork marker) or **(B)** potential induction of a primary stress
953 response promoter (P_{sulA} -yfp reporter). **(C)** Chromosome positioning within the cell is shown in blue
954 (Hoechst dye), relative to the cell membrane in red (NileRed). White arrows indicate an overlap of
955 septation spots (thicker red dots) with DNA (blue) for cells containing λ CI.

956